Optimal Operation of Kaibel Distillation Columns

Maryam Ghadrdan[1], Ivar J. Halvorsen[2] and Sigurd Skogestad[1*]

[1] Department of Chemical Engineering, Norwegian University of Science and Technology, N-7491 Trondheim, Norway, Email: ghadrdan@nt.ntnu.no, skoge@nt.ntnu.no

[2] SINTEF ICT, Applied Cybernetics, N-7465 Trondheim, Norway, Email: ivar.j.halvorsen@sintef.no

Abstract

The objective of this paper is to study the Kaibel distillation column from an operability point of view. Two different objectives, namely minimizing energy requirement at fixed product purities and maximizing product purities with a fixed boilup are considered. We have visualized the objective functions for the two cases as a function of operational degrees of freedom and conclude that operation with fixed product purities is the more difficult case from control point of view.

Keywords: Kaibel column, thermally coupled distillation columns, optimal operation

1. Introduction

The so-called Petlyuk (Petlyuk et al., 1965) distillation configuration separates the feed into three products in a prefractionator-sidestream arrangement with a direct coupling of vapor and liquid streams between prefractionator and main column. The arrangement has only a single reboiler and a single condenser. The divided-wall column (DWC) realizes the Petlyuk configuration in a single shell. This arrangement can be further generalized by adding a

---

* Corresponding author

second side stream to give the Kaibel (Kaibel, 1987) arrangement which is capable of separating four products with a single reboiler and condenser. This tight integration makes it challenging to design and control the column, compared to the conventional sequence of simple columns. The design challenges have been mostly solved, but operation and control remains largely an open issue.

There are two main issues in terms of operation and control. First, the column, and in particular the column profile, needs to be "stabilized" to avoid drift (Strandberg and Skogestad, 2006). This dynamic issue is not studied in this paper. Second, the column needs to be operated as close to its optimum as possible in terms of minimum energy. This is mainly a steady-state issue and is the focus of this paper. It is important because a main motivation behind the Kaibel column is to save energy. Figure 1 and Table 1 show the alternatives which can be used for separating 4 products in conventional column arrangements and a comparison with energy requirement in Kaibel arrangement. These are based on minimum energy requirement for the separations with 95% recovery. As an example, in the following, the V_{min} diagrams of all the columns in one of the alternatives – namely direct sequence- are presented in Figure 2. The idea of Vmin diagram is presented by Halvorsen (2001). It can be constructed for any mixture by simulating a column with a large number of stages, but it is most easily constructed for ideal mixtures based on the Underwood equations. The peaks show the energy needed for the sharp split of two consequent components, e.g. A/B, B/C and C/D from the right for four-component system, and the valleys show the energy needed for non-consequent components, i.e. A/C and B/D for four-component system. The down-most valley is for the so-called "preferred split" (Stichlmair, 1988), that is the minimum energy operating point for the A/D split. The diagrams are based on sharp splits and the operating point for each column is shown by a star (*) – which is 95% recovery in our study. Figure 2 (a) shows the V_{min} diagram for the first column. Here, we have a separation between

A and B with 95% recovery. So, the star shows the operating point for column 1. The distillate flow of column 1 is around 25% of the original feed. The next column has a feed of 75% of the original feed and different feed composition. The task of second column is to separate B from C with 95% recovery. The first peak in Figure 2 (b) is because of the nonsharp split in the previous column. In the case of sharp splits, we will have only two peaks for the second column and 1 for the third column. The energy demand for separating the four components will be the sum of V/F_1 in all the columns. The minimum energy requirement for a full extended Petlyuk arrangement is simply given by the highest peak in the Vmin diagram in Figure 2a. Since we have to add the contributions from the peaks in Fig 2b and 2c for obtaining the direct split sequence we clearly see that it is outperformed by the Petlyuk arrangement. For the Kaibel column, the resulting Vmin diagram is shown in Figure 4. The dashed peaks are obtained by computing a new V_{min} diagram for the upper and lower part of the product columns in the prefractionator arrangement shown in Figure 1e, assuming the equivalent liquid fraction obtained with a fully thermally coupled connection from the prefractionator when it performs the sharp AB/CD split.

As it is reported in Table 1, Kaibel column is the winner of all the alternatives from energy requirement point of view. The value reported in the table for Kaibel column comes from the assumption of sharp split between B and C in the prefractionator. In practice, there will be some allowance for the impurities of the key components B and C in top and bottom of prefractionator which leads to even less amount of vapor requirement for the whole column. This can simply be checked by sketching the objective function (here: total amount of vapor fed to the Kaibel column) as a function of impurities in the top and bottom of the prefractionator from a rigorous simulation.
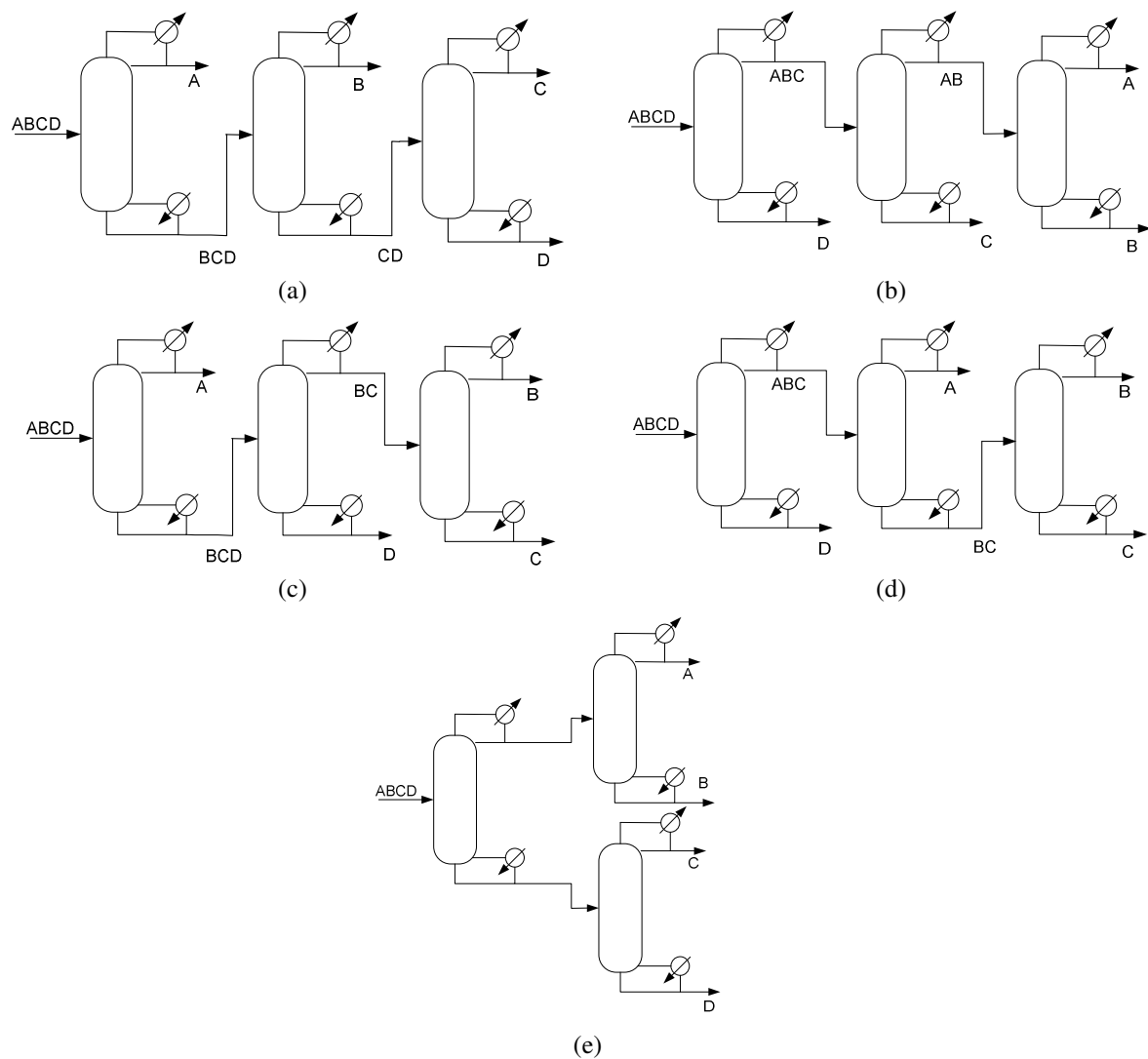
Figure 1. Simple column configuration for a four-component mixture. (a) Direct sequence, (b) Indirect sequence, (c) Direct-Indirect sequence, (d) Indirect-Direct sequence , (e) Prefractionator arrangement

Table 1. Energy requirements for 95% recovery with different simple column configurations and Kaibel arrangement

	V/F for Col1	V/F for Col2.	V/F for Col3.	Sum
Direct Sequence	1.2109	0.6984	0.6133	2.5227
Indirect Sequence	1.1021	0.9471	0.8793	2.9285
Direct-Indirect Sequence	1.2109	0.8732	0.6361	2.7202
Indirect-Direct Sequence	1.1021	0.9372	0.6270	2.6663
Prefractionator	1.0376	0.6137	0.8795	2.5308
Kaibel (Figure 2)				1.8007
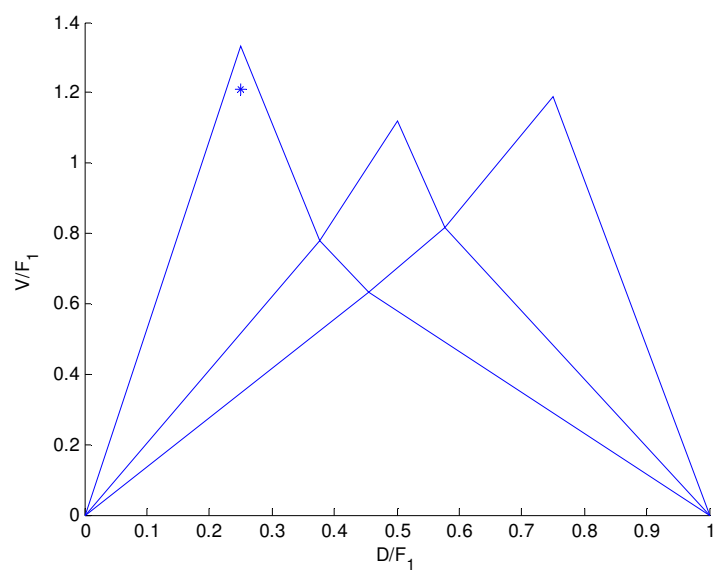
a) V_{min} diagram of Column 1 in Direct sequence
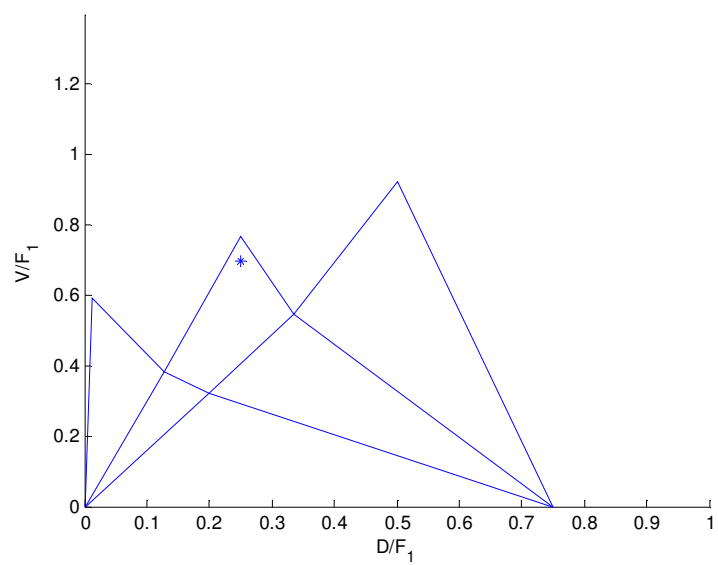
b) V_{min} diagram of Column 2 in Direct sequence
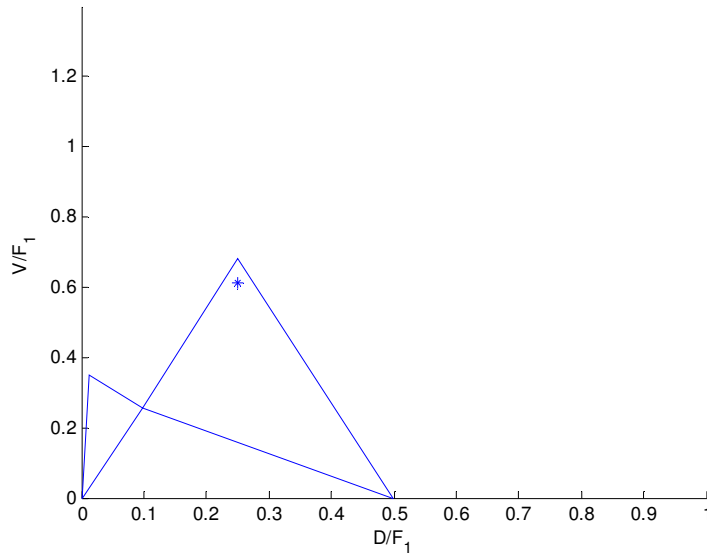
c) V_{min} diagram of Column 3 in Direct sequence

Figure 2. V_{min} diagram for Direct sequence of columns for separating the 4 components under study. The operating point for each column is shown with (*)

In terms of optimal operation, it is usually assumed that the objective is to make products of given purity using the minimum energy. However, in practical operation this is often not the issue, but rather to make the purest possible products with a given energy, especially when there is a bottleneck in the plant. In the paper we discuss both these cases. We are going to study how the mode of operation is going to affect the behavior of the column and as a result the ease of operating the column. Controllability has been studied by some researchers (Diggelen et al., 2010; Ling and Luyben, 2009; Serra et al., 2003) for a three-product dividing wall column. The four-product Kaibel column is more complex and the analysis in this paper addresses the more basic problem of understanding the column behavior at and around the optimal operating point. The insight gained can be used to select a suitable operation target and optimizing control strategy.

So, the two modes of operation which are going to be studied here are as below:

Mode 1. Minimize energy requirement for fixed product purities

Mode 2. Maximize the product purities with constant boilup (ie., minimize impurity sum)

2. System under study

The system under study is shown in Figure 3 and is considered for separation of the first four simple alcohols (Methanol, Ethanol, 1-Propanol, 1-butanol) and the feed is equimolar. Figure 3 (b) shows the schematic of the Kaibel column built in NTNU (Strandberg, 2011). This process is simulated as a 4-column model in UNISIM. It allows flexibility regarding the specifications in different column sections. The pumps and valves are placed to compensate the pressure difference between two column sections in two sides of the wall. In reality different packing structures are used for this purpose. As it is clear from Figure 4 (c), there are 12 trays in each subsection in the main column. The number of trays in the prefractionator is equal to the number of trays in the other side of the wall. It is assumed that the number of trays in all sections are fixed and they are not included in optimization.
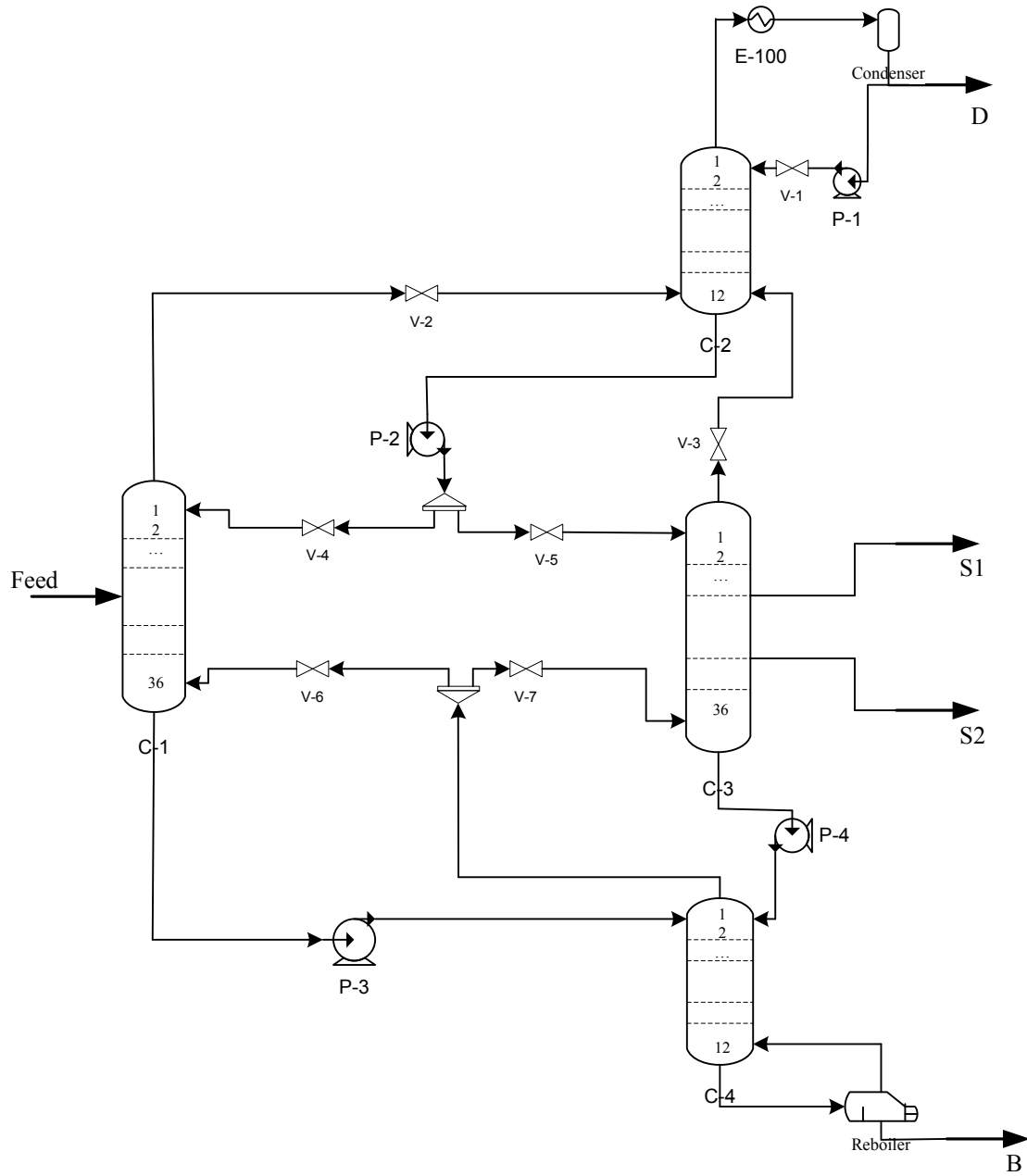
ABCD

A_BCD

_AB_CD

_ABC_D
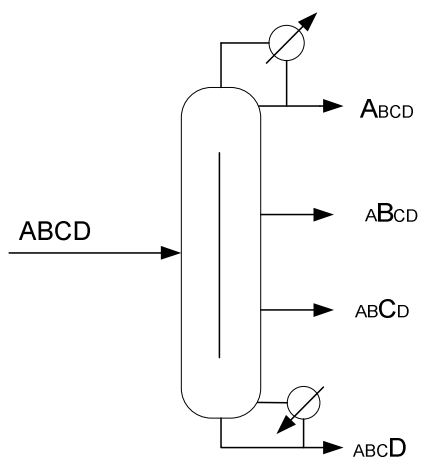
(a)
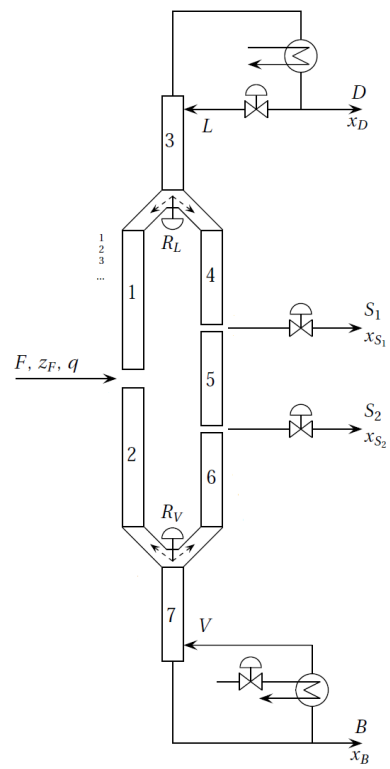
(b)

(c)

Figure 3. (a) 4-Product dividing-wall column schematic, (b) schematic of the lab Kaibel column at NTNU, (c) UNISIM simulation

To achieve the liquid split, a practical solution would be to draw off all liquid above the partitioning wall and transfer it to an intermediate holdup-tank before pumping and metering the liquid back to the column on either side of the dividing wall. Some alternative methods have been reported by the industrial manufacturers (Strandberg and Skogestad, 2010). Note

that liquid split (R_l) is defined as the ratio of the liquid entering the top of the prefractionator to the liquid coming from the top of the main column to the liquid splitter and vapor split (R_v) is defined as the ratio of the vapor entering the bottom of the prefractionator to the vapor entering the vapor splitter from bottom of the main column.

In the case of the vapor split, the situation is quite different. Except for Strandberg (2011), there are no reports of adjustable vapor splits in the literature, nor has it been reported in any industrial implementations. Usually the detailed design will determine the best position of the wall and the pressure drop either side of the partitioning will determine the vapor split ratio. One can argue that if the desired vapor split ratio is not achieved it can be compensated by adjusting the liquid split. This is true up to a point, but if the ratio is too far off from the optimal value the product purities or at least the column efficiency will suffer. However, in case of manipulating vapor split, we have an extra degree of freedom for control that could be used to increase purities or make the separation more energy efficient in the face of process disturbances (Strandberg and Skogestad, 2010).

Figure 4 shows a schematic of the minimum energy diagram for the case under study. For every possible operating point, the normalized vapor flow rate (V/F), the overall product split (D/F or B/F), and the distribution (given by a set of recoveries) is shown. Note that the peaks and valleys are only valid. They are calculated based on the Underwood equations.

The peaks at the dashed lines in Figure 4 give the vapor flow rate requirement to separate A/B and C/D in a Kaibel column, when the prefractionator does a sharp AB/CD split. The highest peak (here P'_{AB}) determines the overall energy requirement of the Kaibel column, so the lower part of the column has more energy available than required. This can be utilized to obtain somewhat higher purity in the other section of the column or to reduce the number of stages. The other point is that unlike Petlyuk configuration where we normally have a certain slack in

the prefractionator operation regarding distribution of the intermediate components (B and C), the Kaibel-column prefractionator must perform a relatively sharp split between streams AB and CD, given by the P_{BC} in the Vmin-diagram. We can find a certain slack if we allow nonsharp split in Kaibel configuration, but this is limited by the product specifications. Prefractionator operation with higher vapor rate than at P_{BC} could give us some slack also for sharp AB/CD split, but this will lead to higher vapor requirement to split A/B and C/D in the succeeding sections.
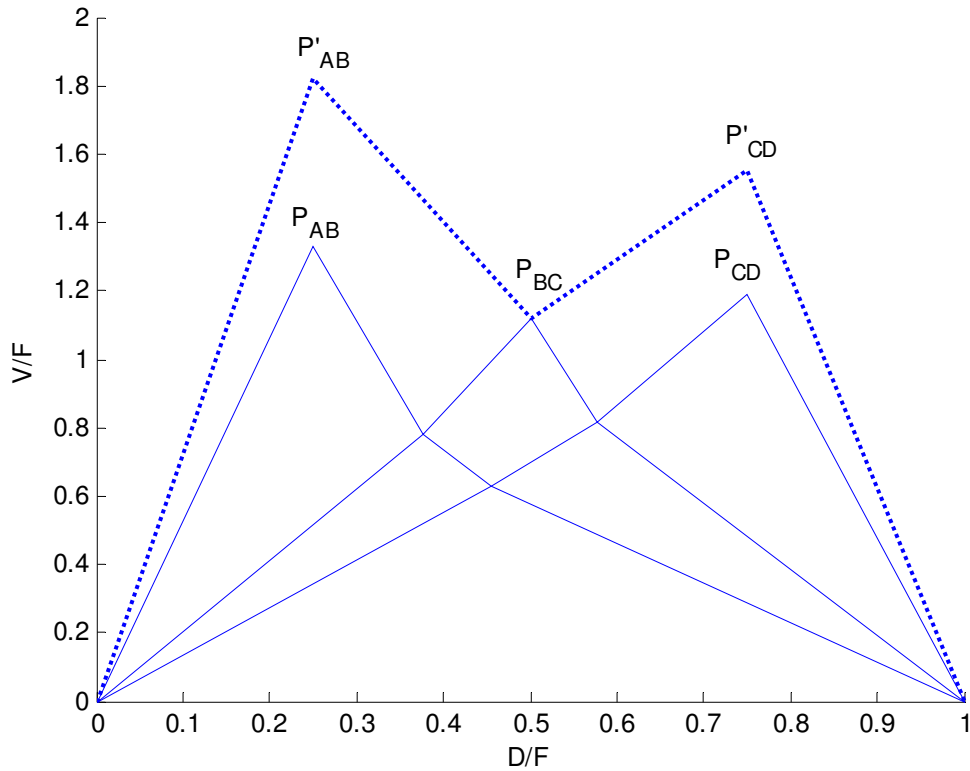
Figure 4. Minimum energy diagram (solid lines) for the equimolar mixture of Methanol, Ethanol, 1-Propanol, 1-Butanol (Halvorsen and Skogestad, 2006). The highest peak (P_{AB}) gives te minimum boilup for petlyuk arrangement. The dotted line is for the Kaibel column and the highest peak (P'_{AB}) gives the minimum biolup

Figure 5 shows the structure which is used for obtaining good estimates for flows as initial values using the information from Vmin-diagram. The number of degrees of freedom in this

structure is again 6 and all of them are for the main column (four product compositions and two flowrates of the streams going back to the prefractionator). We use the minimum rates from minimum energy diagram together with the pinch point compositions (Halvorsen, 2001) at the ends of the prefractionator from the ideal model as an initial guess. The flow rates and compositions of the returning streams (R2 and VB2) to the prefractionator should match the ones entering the the prefractionator column (R1 and VB1). So, by setting the compositions of the entering streams (R1 and VB1) from pinch point calculations, and the flow rates of the returning streams from the Vmin diagram, we'll have some iteration to adjust the flow rates of the entering streams, so that the compositions of the returning streams match the ones of the entering streams. The split values from this simulation are used in the original model to find the minimum energy required for the separation. This model is mainly used for the cases where we had problem in convergence, especially for the mode of minimizing energy requirement.
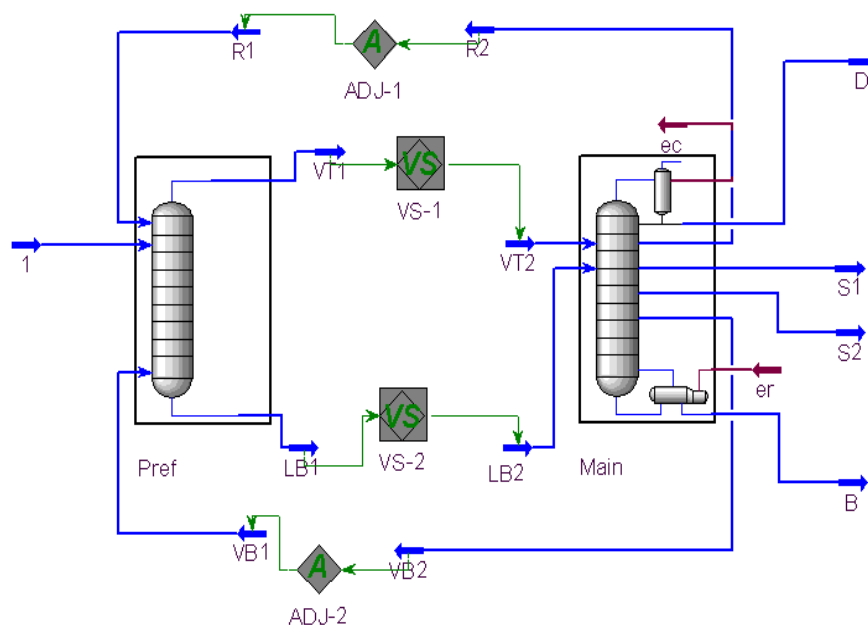

Figure 5. UNISIM simulation that uses the information from V_{min} diagram to obtain initial estimates for the detailed simulation

3. Minimize energy requirement (mode 1)

The objective is here to minimize the energy requirement with given purities of the four products. The cost function J to be minimized is therefore selected to be the boilup rate

$$J = V$$

For mode 1 where the products purities are fixed, there remain two degrees of freedom (vapor and liquid splits) which should be used to minimize energy requirement. The other degrees of freedom are used to satisfy the product purities specifications. Since the product purities are constraints, the splits are inter-related and cannot be changed independently as optimization variables to get to the minimum energy requirement. So, it is difficult to run the optimization program as it is done for the other mode. Therefore, to get a feeling about where the optimum is, the minimum vapor rates is found from the Vmin-diagram (Halvorsen and Skogestad, 2006). Figure 6 shows the optimal composition and temperature profiles for the nominal case and different disturbances. We will discuss about Figure 6 (b) more in the next section.
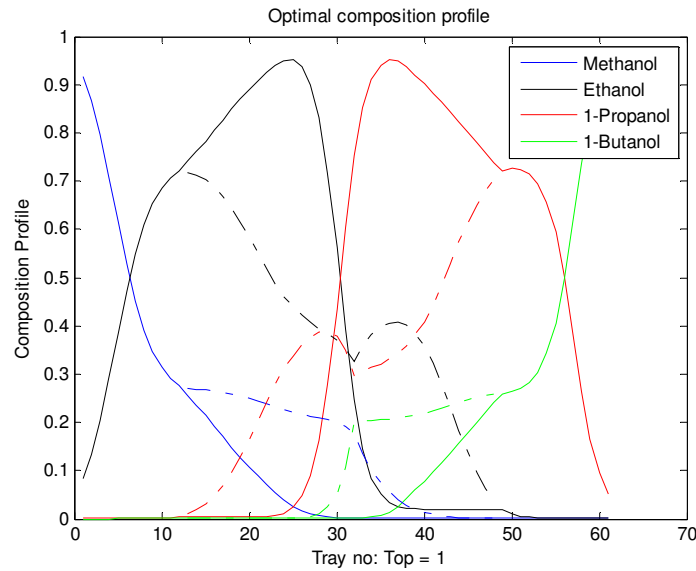

(a)
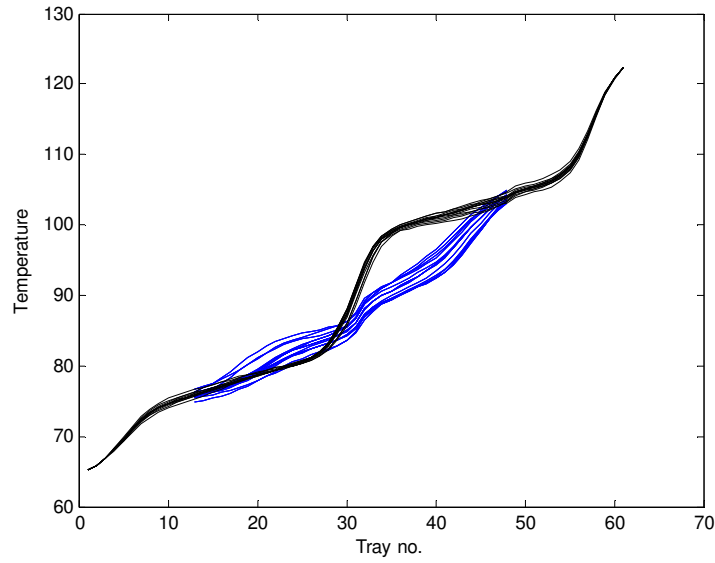
(b)

Figure 6. Mode 1: Optimal composition and temperature profiles

(a) Optimal composition profile for nominal case – Prefractionator: dashed lines, main column: solid

lines. (feed liquid fraction = 1)

(b) Optimal temperature profiles for nominal case and various disturbances in feed compositions

(5%), liquid fraction (10%) and feed flowrate 10%) – Prefractionator: blue lines, main column:

black lines. (feed liquid fraction = 1)

Visualization of the cost function gives a qualitative insight into the problem at hand. Since there are two optimization variables, the solution surfaces can be shown in 2-dimentional plots. The contours of the objective value are shown in Figure 7. In the 3-dimentional graph, they are like thin bended cones. The cross-sectional area of the cone will increase as boilup flow rate increases. This figure also shows that for the case which feed quality is zero, R_l is greater than R_v, especially near the optimal point. The opposite is seen for for the case of q=1. The reason is quite obvious (e.g. for q = 0, since a part of vapor needed for separation is provided by the feed itself, so it needs more liquid than vapor to contact). Note that this can not be generalized. For other feed compositions or relative volatilities, this is not followed.
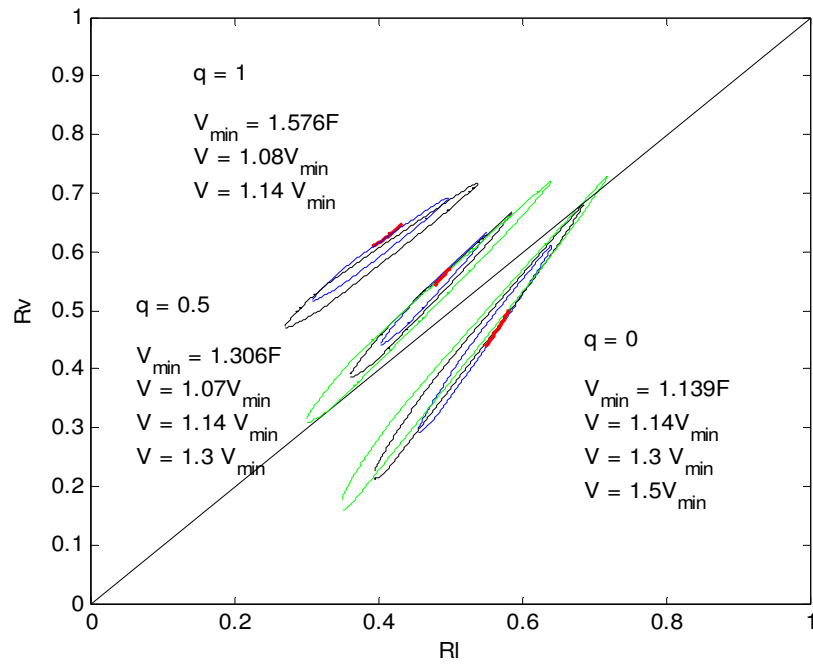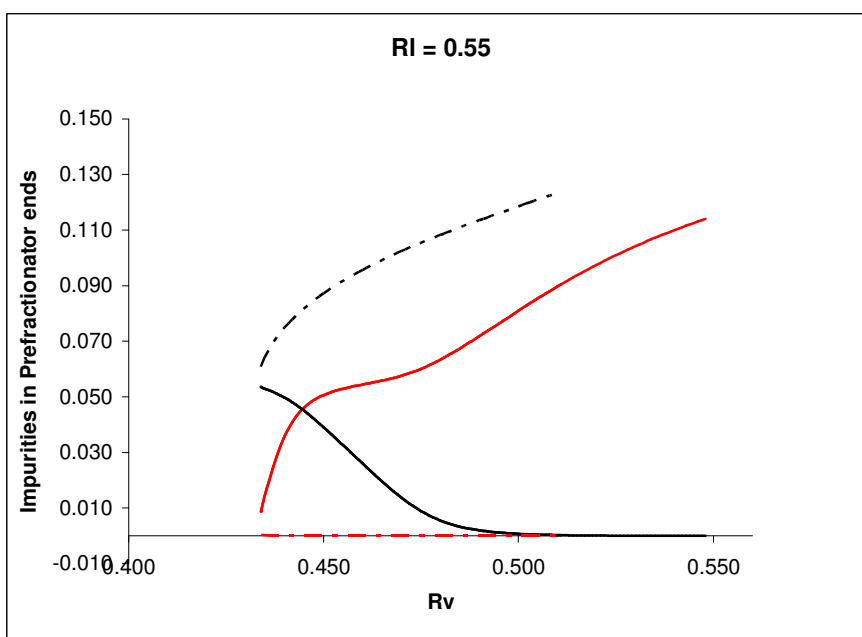
Figure 7. Mode 1 (fixed purities of 95% for all products): Contours of boilup as a function of liquid and vapor splits for liquid feed (q = 1), two-phase feed (q = 0.5) and vapor feed (q = 0)

There exists multiplicity in the solution. This can be seen in Figure 8 (a) as we get two different boilups when all the specifications are set and the system is defined. This is due to two different ways for impurity flows to go to products (Wolff and Skogestad, 1995) - namely from top or bottom of the prefractionator (see Figure 8 (b)).
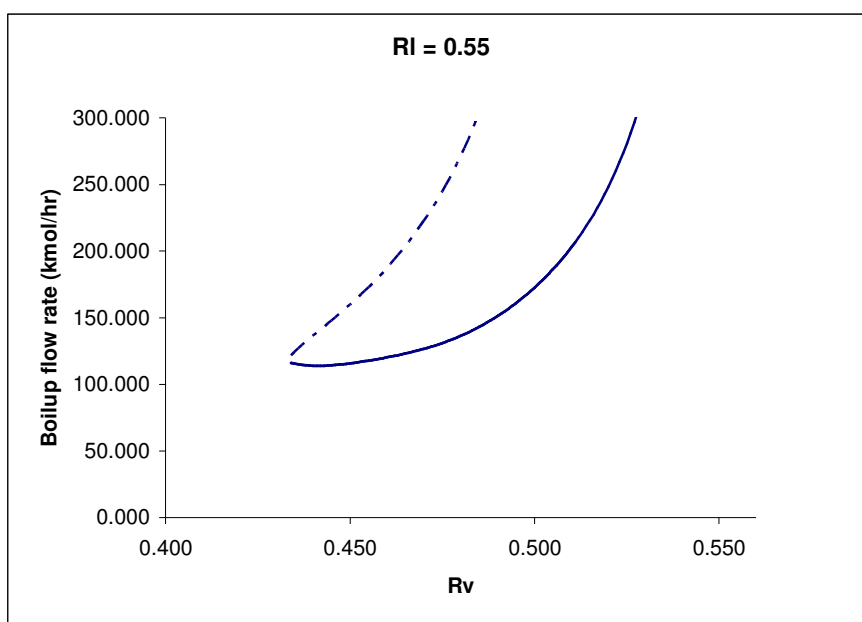
(a)

(b)

Figure 8. Mode 1 (fixed purities of 95% for all products): (a) Boilup rate as a function of vapor split (R_v) with fixed liquid split.

(b) Impurities of C2 and C3 in the ends of prefractionator, red for C3 and black for C2 respectively.

The solid lines in figure (a) correspond to the solid line in figure (b). (Feed liquid fraction = 0)

Figure 9 shows the dependency of boilup rate on the vapor split as the liquid split changes over a wide range. It shows the general trend of change of the minimum vapor as the splits are changing and the span for one split value in which there is a feasible solution as the other one is fixed. Also, the location of minimum is clearer in this figure.
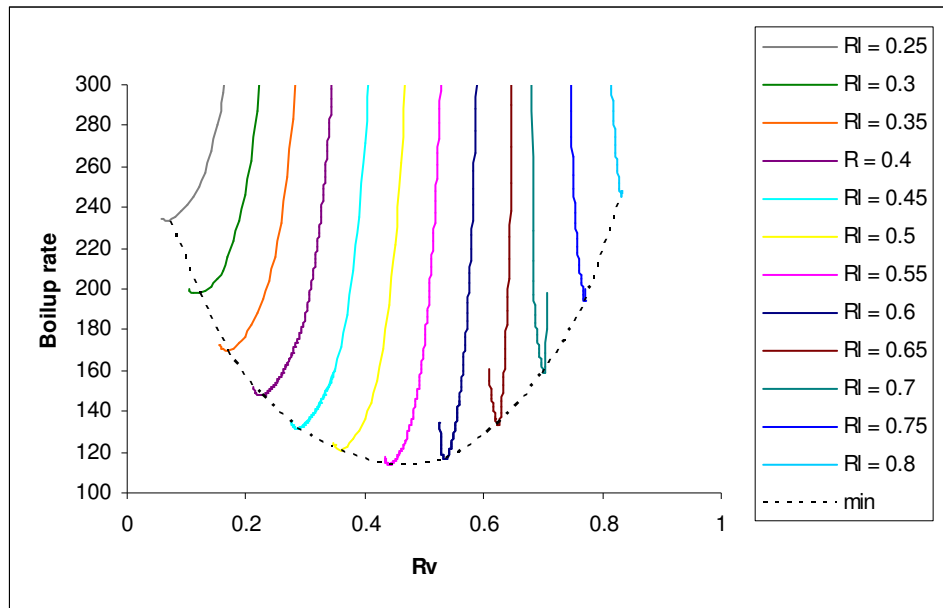
Figure 9. Mode 1 (fixed purities of 95% for all products): Boilup rate versus vapor split (R_v) at different values of liquid split (Feed liquid fraction = 0)

As mentioned previously, in industrial practice it is not common to adjust the vapor split online. It will normally be given by the dividing wall placement and flow/pressure characteristics of the packings and the liquid load on each side. The results show that the optimal operating region (somewhat close to minimum energy point) is narrow and we are actually forcing the process to go through a very restricted area to reach the purity specifications. So, the liquid split has to be adjusted carefully to obtain minimum energy.

4. Maximize product purities with fixed boilup rate (mode 2)

The objective function is here to maximize the purity of the products with a given energy, that is, with fixed boilup (V). The cost function J to be minimized can be defined as the sum of the impurities in the products,

$$J = D\left(1-x_D\right) + S1\left(1-x_{S1}\right) + S2\left(1-x_{S2}\right) + B\left(1-x_B\right)$$

Two different cases that will lead to this mode are (Strandberg and Skogestad, 2010):

1. If all the prices for the products are equal, but we get paid for the main component only in each product.

2. If products S_1 (upper side stream) and B (bottom product) have zero value (or same value as the feed) and for the valuable products S_2 and D we only get paid for the main component. In this case all impurities give losses.

The optimal steady state solution is reached with a specified boilup rate and with the other degrees of freedom optimized such that the products will be as pure as possible. Table 2 shows the results of optimization for the two cases studied in this paper. The numbers in bold in each column are fixed during the optimization. The optimal composition and temperature profiles for the nominal case and different disturbances are shown below (Figure 10). It is seen that optimally the temperatures in the middle trays (trays 15-33) of main column and middle of the prefractionator remain constant after applying disturbances. So, these temperatures are good candidates as controlled variables. Combinations of measurements which show self-optimizing properties can also be considered as controlled variables (Alstad et al., 2009).

Note that it is possible to increase some of the products purities with the same amount of energy (vapor). Some of the products will easier obtain higher purity than the other, which is

due to both the actual selected number of stages and to the extra energy available in the parts of the column related to the lowest peak in the Vmin-diagram (here the bottom split related to P'_{CD}). Thus, this should be considered when specifying the individual product purities with the minimum energy objective since only the most difficult split is actually setting the energy requirement.
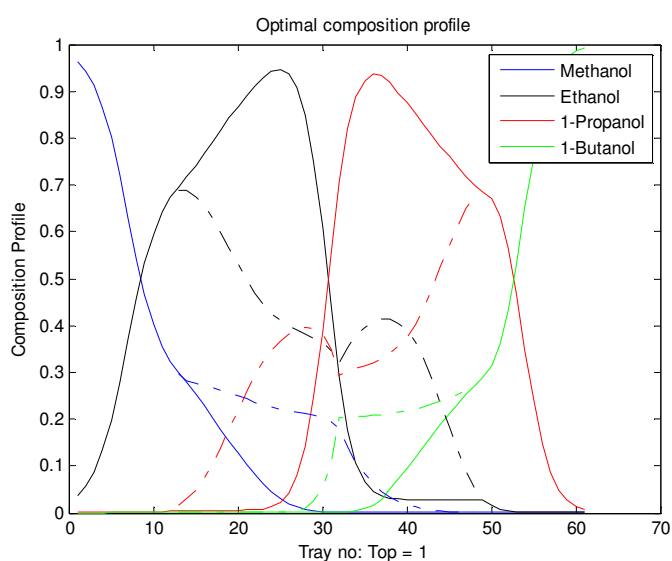
(a)
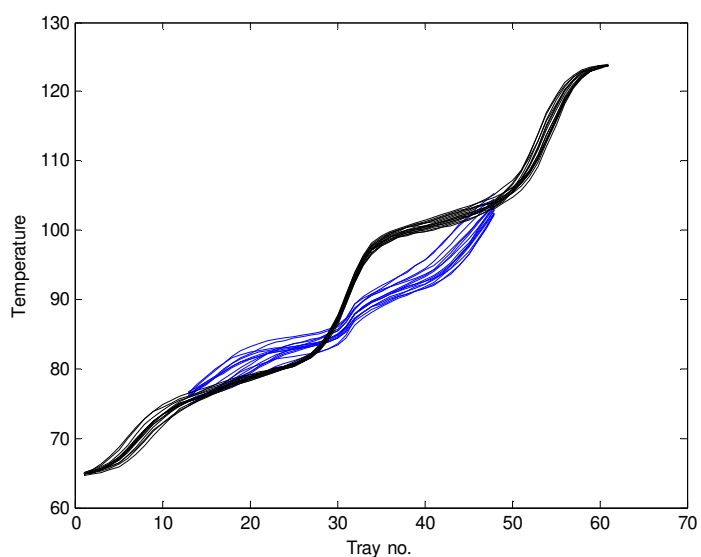
(b)

**Figure 10.** Mode 2: Optimal composition and temperature profiles for nominal case

(a) Optimal composition profile for nominal case – Prefractionator: dashed lines, main column: solid lines. (feed quality = 1)

(b) Optimal temperature profiles for nominal case and various disturbances in feed compositions (5%), liquid fraction (10%), boilup flow setpoint (10%) and feed flowrate 10%) – Prefractionator: blue lines, main column: black lines. (feed quality = 1)

Table 2. Optimal steady-state solution (equimolar feed of 100kmol/hr which is saturated liquid)

	Mode 1 (minimize V with fixed purities)	Mode 2 (maximize product purities with fixed V)
R_L	0.42	0.4009
R_V	0.635	0.6179
Reflux Ratio	6.127	6.375
D flow rate (kmol/h)	25.33	24.43
B flow rate (kmol/h)	25.68	24.41
S_1 flow rate (kmol/h)	24.32	24.93
S_2 flow rate (kmol/h)	24.67	26.22
V (kmol/h)	157	**157**
Q (kW)	1842	**1842**
Objective value	157	0.00108
Purity of Methanol in D	**95%**	97.66
Purity of Ethanol in S_1	**95%**	94.19
Purity of 1-Propanol in S_2	**95%**	93.48
Purity of 1-Butanol in B	**95%**	99.28

For control purposes it is interesting to know how the manipulated variables affect the process. Figure 11 shows the dependency of product compositions and the objective value on each of the five degrees of freedom while all the others are kept constant at their nominal point. The objective value shows a linear dependency on the variables away from the optimum. The degree of effect of a change in each variable on the objective value is clear in these figures. For example, the deviation of S_1 from the optimal point has more effect on the objective value than S_2. It can be seen that any change in reflux (L) and side streams flow rates (S_1, S_2) affect mainly the purities below. For example a change in the S_1 flow rate does not have any effect on the purity of the distillate stream. Likewise, the change in S_2 flow rate does not have any effect on the purity of the distillate and S_1 streams. By considering each of the four parts as separate columns, we can easily confirm the results by analyzing the amounts of internal flows in each part and how they affect separation. Often in distillation, the internal flows, reflux and boilup, are used as control degrees of freedom.
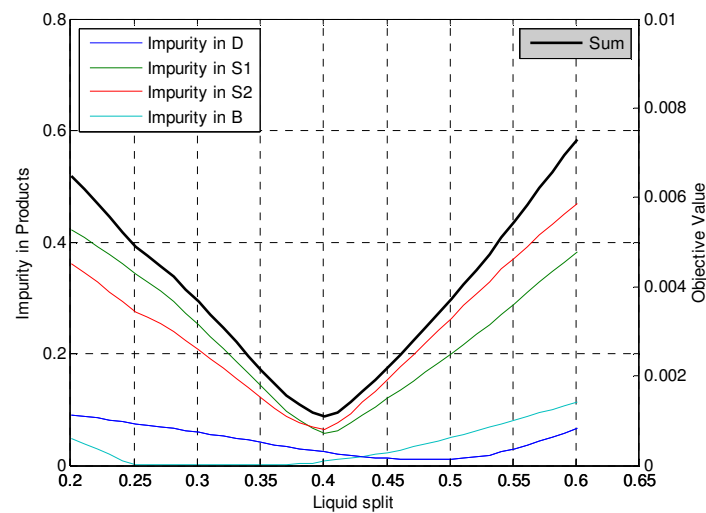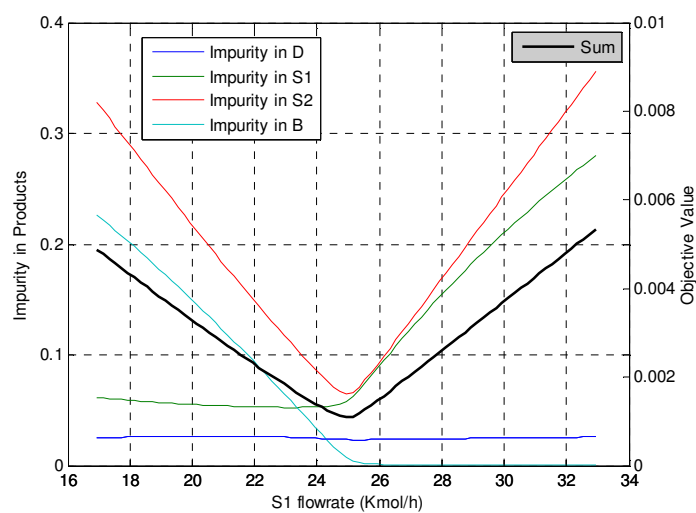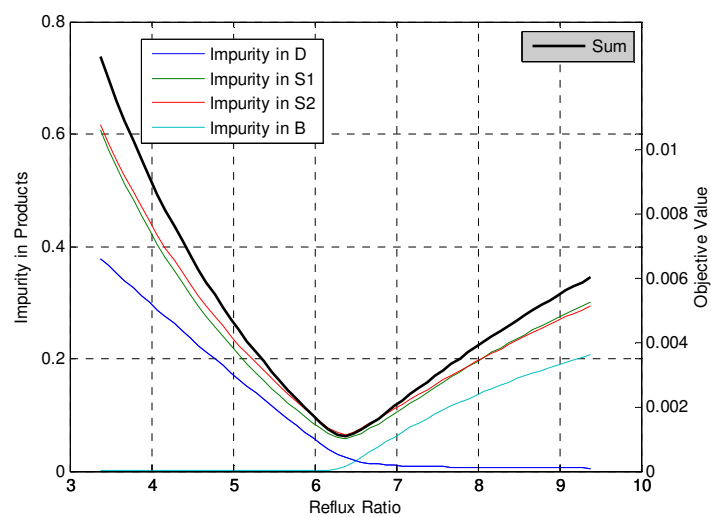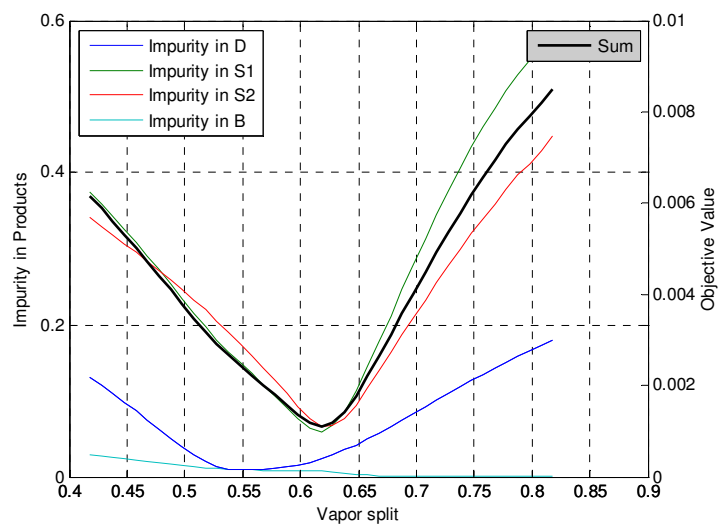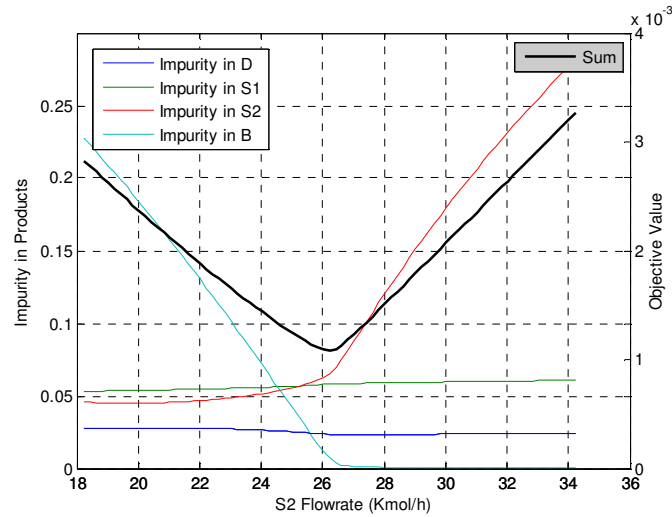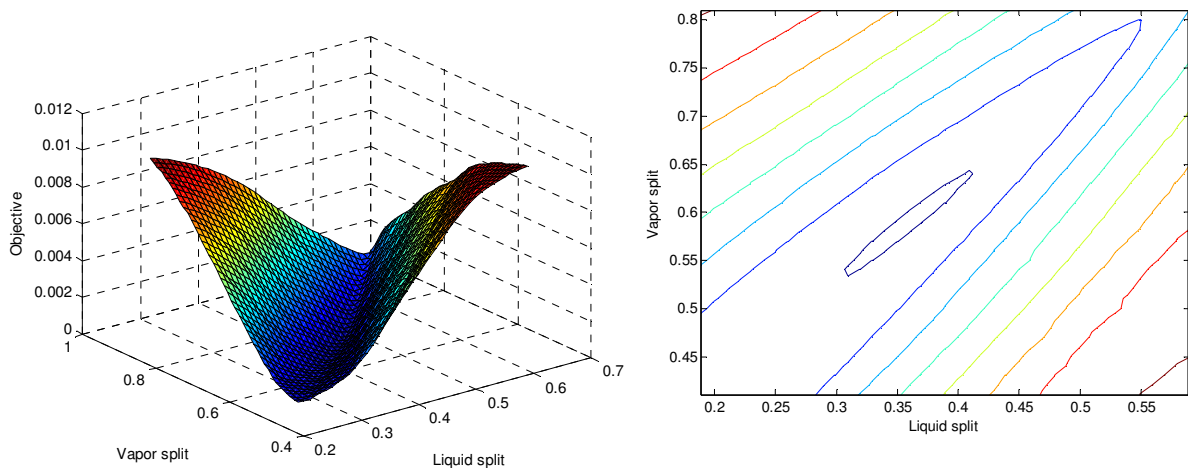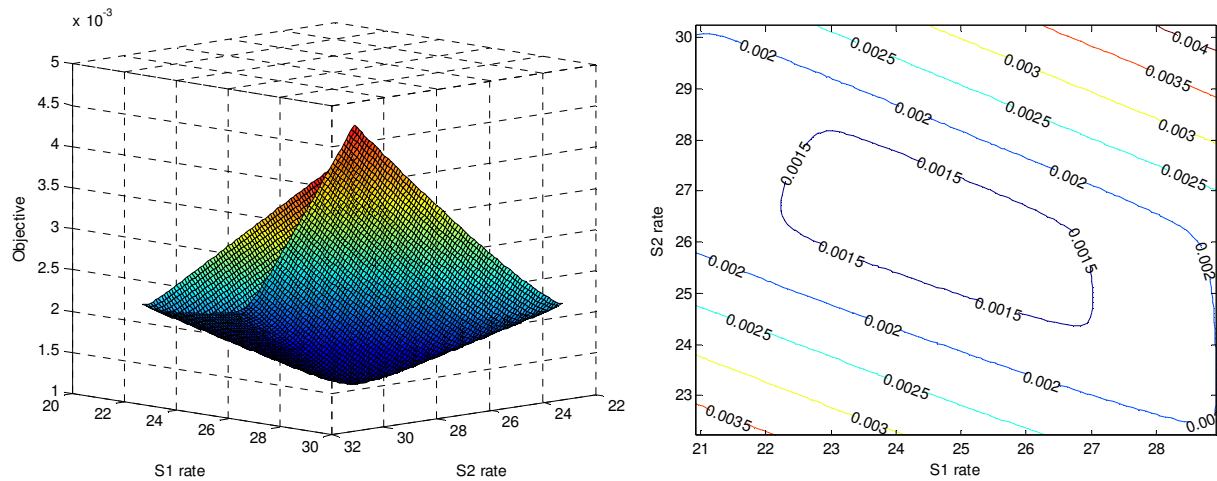
Figure 11. Mode 2 with fixed boilup: Impurities in each product and sum (cost J) as a function of the degrees of freedom (vapor split, liquid split, reflux, side stream flow rates) with the other variables kept constant at their original optimal values.

Since there are five degrees of freedom, it is difficult to sketch the solution surface in this case. Figure 12 includes 3-dimensional surfaces which show how the objective value is affected by splits and side stream flow changes. Like the previous case, there is "bad" direction for both of them, along which a small change in one of the variables will result in a large change in the objective value.

Figure 12. Mode 2 with fixed boilup: 3-D surfaces and contour plot of impurity sum (cost J) as a function of degrees of freedom with the other variables fixed at their optimal values

5. Conclusions

In this paper, two alternatives for operating a Kaibel column are studied. By comparing two modes of operation, it is shown that the first mode, which is minimizing vapor flow rate at constant product purities, is the more difficult case to handle. This difficulty is due to the very narrow solution surface and also multiplicity problem. However, the second mode, where the product purities are free, seems to be easier to operate. This case is not as common as the first objective, but can be relevant for refineries where the product purities do not play vital role or when there is a bottleneck in the process.

References

Alstad, V., Skogestad, S., Hori, E.S., 2009. Optimal measurement combinations as controlled variables. Journal of Process Control 19, 138-148.

Diggelen, R.C.v., Kiss, A.A., Heemink, A.W., 2010. Comparison of Control Strategies for Dividing-Wall Columns. Ind. Eng. Chem. Res. 49, 288-307.

Halvorsen, I.J., 2001. Minimum Energy Requirements in Complex Distillation Arrangements. Norwegian University of Science and Technology, Department of Chemical Engineering (Available from home page of S. Skogestad).

Halvorsen, I.J., Skogestad, S., 2006. Minimum Energy for the four-product Kaibel-column AIChE Annual meeting 2006, San Francisco p. 216d

Kaibel, G., 1987. Distillation columns with vertical partitions. Chem. Eng. Technol. 10.

Ling, H., Luyben, W.L., 2009. New Control Structure for Divided-Wall Columns. Ind. Eng. Chem. Res. 48 6034-6049.

Petlyuk, F.B., Platonov, V.M., Slavinskii, D.M., 1965. Thermodynamically optimal method for separating multicomponent mixtures. Int. Chem. Eng., 555-561.

Serra, M., Espuña, A., Puigjaner, L., 2003. Controllability of Different Multicomponent Distillation Arrangements. Ind. Eng. Chem. Res. 42, 1773-1782.

Stichlmair, J., 1988. Distillation and Rectification, Ullmann's Encyclopedia of Industrial Chemistry. Wiley-VCH.

Strandberg, J., Skogestad, S., 2006. Stabilizing Control of an Integrated 4-Product Kaibel Column, ADCHEM Gramado, Brazil.

Strandberg, J., Skogestad, S., 2010. Basic Control of Dividing-wall Columns, DA2010, Eindhoven, the Netherlands.

Strandberg, J.P., 2011. Optimal operation of dividing wall columns. Norwegian University of Science and Technology, Department of Chemical Engineering (available from home page of S. Skogestad).

Wolff, E.A., Skogestad, S., 1995. Operation of integrated three-product (Petlyuk) distillation columns. Ind. Eng. Chem. Res. 34, 2094-2103.